THE ASTROPHYSICAL JOURNAL, 530:L53–L56, 2000 February 20

YOUNG RED SPHEROIDAL GALAXIES IN THE HUBBLE DEEP FIELDS:[1,2,3] EVIDENCE FOR A TRUNCATED INITIAL MASS FUNCTION AT ∼2 $M_\odot$ AND A CONSTANT SPACE DENSITY TO $z \sim 2$

TOM BROADHURST[4,5] AND RYCHARD J. BOUWENS[5]

Received 1999 March 9; accepted 1999 December 23; published 2000 January 31

ABSTRACT

The optical-IR images of the northern and southern Hubble Deep Fields are used to measure the spectral and density evolution of early-type galaxies. The mean spectral energy distribution is found to evolve passively toward a mid-F star–dominated spectrum by $z \sim 2$, becoming more sharply peaked around the 4000 Å break. We demonstrate with realistic simulations that hotter elliptical galaxies would be readily visible if evolution progressed blueward and brightward at $z > 2$, following a standard initial mass function (IMF). The color distributions are best fitted by a "red" IMF, deficient above ∼2 $M_\odot$ and with a spread of formation in the range $1.5 < z_f < 2.5$. Traditional age dating is spurious in this context; a distant elliptical can be young but appear red, with an apparent age greater than 3 Gyr independent of its formation redshift. Regarding density evolution, we demonstrate that the sharp decline in numbers claimed at $z > 1$ results from a selection bias against distant red galaxies in the optical, where the flux is too weak for morphological classification, but is remedied with relatively modest IR exposures that reveal a roughly constant space density to $z \sim 2$, with 32 and 16 elliptical galaxies detected above and below $z = 1$, respectively. We point out that the lack of high-mass star formation inferred here and the requirement of metals implicates cooling flows of preenriched gas in the creation of the *stellar* content of spheroidal galaxies. Deep-field X-ray images will be very helpful in examining this possibility.

Subject headings: cosmology: observations — galaxies: distances and redshifts — galaxies: elliptical and lenticular, cD — galaxies: formation

1. INTRODUCTION

Elliptical galaxies are anomalous in many respects when considered in the context of the standard ideas regarding galaxy and star formation. Despite the absence of star formation today, only minimal passive evolution has been identified to $z \sim 1$, mainly from optical-IR colors of cluster sequences, which are marginally bluer than *k*-corrections predict (Stanford, Eisenhardt, & Dickinson 1998). At higher redshift, examples of luminous red galaxies are found with F and G star–dominated spectra (Dunlop et al. 1996; Peacock et al. 1998). No bright blue precursors have been identified. The absence of precursors naively implies that the early epoch was obscured by dust or restricted to unobservably high redshifts. Benitez et al. (1999) strongly limit any unobscured formation to $z > 10$ in the deepest available VLT/NICMOS images.

In the context of hierarchical models, it is natural to view E/S0 galaxies as the end product of a merging process and hence to predict declining numbers with increasing redshift. Locally at least, merging of disk galaxies is seen to create some spheroidal-shaped objects (Schweizer & Seitzer 1992). At faint magnitudes, claims have been made for a decline in the space density of red and/or elliptical galaxies at $z > 1$ (Kauffmann, Charlot, & White 1996; Zepf 1997; Franceschini et al. 1998; Kauffmann & Charlot 1998; Menanteau et al. 1999; Barger et al. 1999). Conflicting with this is the simplicity of structural and color relations between elliptical galaxies (Faber & Jackson 1976), particularly in rich clusters in which coeval formation is inferred (Bower, Lucey, & Ellis 1992).

If gas-rich mergers of spiral galaxies are to produce the elliptical galaxies, then the enhanced alpha-element abundance generated by a brief merger induced episode of star formation is unacceptably diluted by the preexisting Type Ia supernova–enriched ISM (Thomas, Greggio, & Bender 1999). Furthermore, the mass of stars formed during a merger is limited by the general absence of an intermediate-age stellar population in postmerger elliptical galaxies (Silva & Bothun 1998; James & Mobasher 1999). Metallicity is also a problem with monolithic collapse formation, as closed-box star formation does not account for the observed lack of low-metallicity stars (Worthey 1994) but implies preenrichment of the gas (Thomas et al. 1999).

Recently, distant red elliptical galaxies and other spheroid-dominated galaxies at $1 < z < 2$ have been detected in the deepest combination of optical-IR images—a small NICMOS/VLT field (Benitez et al. 1999; Treu et al. 1998; Stiavelli et al. 1999). Here we analyze a much larger sample of distant red galaxies by combining optical-IR photometry from both Hubble Deep Fields to measure the rates of spectral and density evolution (§§ 3 and 4) with photometric redshift measurements (§ 2) and discuss new implications for their formation (§ 4).

2. OBSERVATIONS

The observations used here are the deep *Hubble Space Telescope* (*HST*) optical images in the *UBVI* (Williams et al. 1996; R. Williams et al. 2000, in preparation) and the *JHK* images from KPNO (Dickinson et al. 1997)[6] and from the SOFI in-

[1] Based on observations made with NASA/ESA *Hubble Space Telescope*, which is operated by AURA, Inc., under contract with NASA.

[2] Based on observations made at the Kitt Peak National Observatory, National Optical Astronomy Observatories, which is operated by the Association of Universities for Research in Astronomy (AURA), Inc., under cooperative agreement with the National Science Foundation.

[3] Observations have been carried out using the ESO New Technology Telescope at the La Silla observatory under program numbers 59.A-9005(A) and 60.A-9005(A).

[4] European Southern Observatory, Karl-Schwarzschild-Strasse 2, Garching bei München, D-85748 Germany.

[5] Department of Astronomy, University of California, Berkeley, Berkeley, CA 94720.

[6] Available at http://archive.stsci.edu/hdf/hdfirim.html.

strument on the New Technology Telescope (NTT) in the south (da Costa et al. 1999). We use the published zero points, filter transmission, and detector response curves. Magnitudes are measured using SExtractor (Bertin & Arnouts 1996), and photometric redshifts are estimated by maximizing the likelihood with respect to a set of instantaneous burst spectra calculated using the $[Z/Z_{\odot}] = -0.2$ Bruzual/Charlot spectrophotometric package (Leitherer et al. 1996). Stars are distinguishable to very faint magnitudes by both a stellarity index (Bertin & Arnouts 1996) and, interestingly for red stars, by a poor fit to redshifted red galaxy spectra.

3. SPECTRAL EVOLUTION

The first point to note is that the choice of metallicity does not significantly affect the redshift estimate. The break at 4000 Å is so sharp that with accurate optical-IR magnitudes the redshift can be determined to ∼15% by eye. A comparison of photometric redshifts with the 10 spectroscopic redshifts of elliptical galaxies in the HDF North is very good with a hint of a $\delta z = 0.1$ systematic overestimate. Our 48 galaxy elliptical sample was chosen from the combined *HST* deep field and ground-based IR-photometry. The sample is the union of those objects with well-fitted *I*-band de Vaucouleurs profiles and those objects with red colors consistent with passive evolution. We included a few objects for which the *I*-band flux is too faint to reliably discriminate between an exponential and a de Vaucouleurs profile, but for which the optical-IR colors clearly show that the spectral shape is early type. However, most objects in our sample (39) lie in the intersection of these two classes, i.e., being well fit both spectroscopically and morphologically.

The spectral energy distributions (SEDs) are compared in the rest frame (Fig. 1). A clear evolutionary trend emerges toward a mid-F star–dominated spectrum by $z \sim 2$. Hotter A star–dominated spectra would be very easily recognized if elliptical galaxies evolved further according to a standard initial mass function (IMF) at $z > 2$, such young (<1 Gyr) precursors being very bright and blue. This simple result suggests that the passive evolution of elliptical galaxies begins at $\sim 2\ M_{\odot}$. For approximately ∼1–2 Gyr after formation, the spectrum of such a stellar population has no detectable spectral evolution, consistent with the slow evolution found here above $z \sim 1$ (Fig. 1). This level of evolution corresponds to a change of 1.2 mag in rest-frame *B* between $z \sim 2$ and the present. A small but detectable variance among SEDs is observed at any redshift (Fig. 1) with evidence for greater homogeneity at high redshift. It is unlikely this early blue phase would lie at unobservably high redshifts since adding 1 Gyr to $z \sim 2$ corresponds to a redshift of only $z = 4.5$ in the worst case, $\Omega = 1$, $H_0 = 70$ km s^{-1} Mpc^{-1} model, and more reasonably with $\Omega = 0.1$, $H_0 = 70$ km s^{-1} Mpc^{-1} corresponding to a formation redshift of only $z = 2.8$.

The bluest three objects marking the starting point of the color-color tracks in Figure 3 have accurate estimated redshifts in the range $1 < z < 2$. These objects contain a small blue excess in *U* and *B* relative to an F star spectrum (Fig. 2, *bottom*) which is spatially distributed like the general light profile (Fig. 2), ruling out a contribution from an active nucleus. Accommodating this with some A star light steepens the IR appreciably, requiring a redder IMF for a good fit. Nebular continuum emission is an interesting possibility. Spectroscopy would be very helpful in understanding these relatively blue elliptical galaxies.

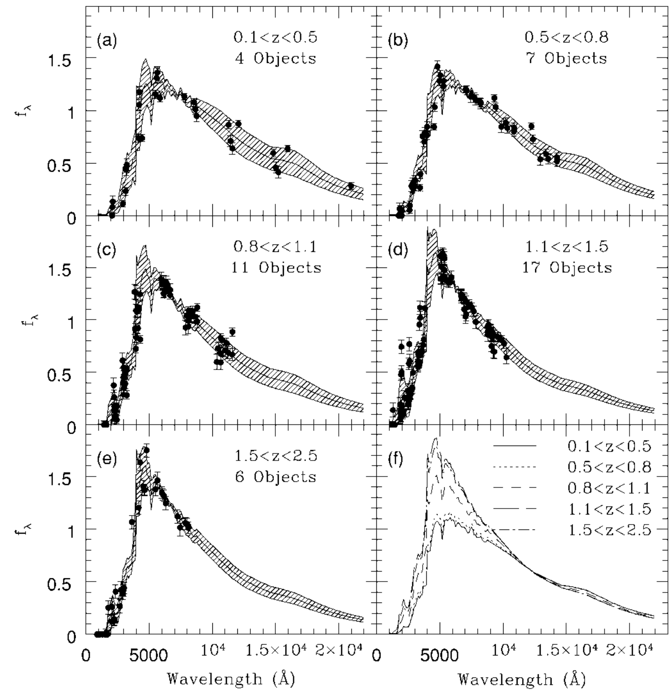

FIG. 1.—Spectral evolution of the early-type galaxies can be traced with redshift via their mean SEDs (*a*–*e*) in the range $z < 2.5$. A detectable variance between SEDs is apparent at all redshifts but a general smooth trend is apparent toward the peaked shape so typical of an F star–dominated spectrum. Panel (*f*) shows the trend of the mean model SED over the full redshift range normalized in the red. Surprisingly, nothing bluer than a mid-type F star–dominated spectrum is found.

4. DENSITY EVOLUTION

A proper assessment of density evolution requires simulated images to account for the very strong redshift-dependent *k*-correction. Simulations are made in all bands using the local luminosity function of early-type galaxies (Pozzetti, Bruzual, & Zamorani 1996) and matched in background noise, pixel scale, and point-spread function (PSF) of each passband, using a variation of the machinery described in Bouwens, Broadhurst, & Silk (1998). Selection and photometry of both the observed and simulated images are performed identically. Figure 3 shows a comparison with a model in which the density is fixed and only the observed spectral evolution takes place to $z_f = 2.5$. It is clear that the numbers and luminosities of red galaxies have not changed much between $z \sim 2$ and the present, in agreement with the claim of Benitez et al. (1999), but inconsistent with other estimates, in particular previous optical work. The unknown volume at high redshift translates into an uncertainty in the predicted numbers at $z > 1$, so that both low Ω and flat Λ–dominated models overpredict the data by ∼30%.

5. DISCUSSION AND CONCLUSIONS

Our findings show that the passive evolution of elliptical galaxies evolves slowly to a mid-F star spectrum by $z \sim 2$. Bluer elliptical galaxies are conspicuous by their absence, and at face value, this simply suggests that the main sequence in elliptical galaxies does not extend above $\sim 2\ M_{\odot}$. It is also clear that most elliptical galaxies form at $z > 1$ given the lack of any significant decline in their space density with redshift, although

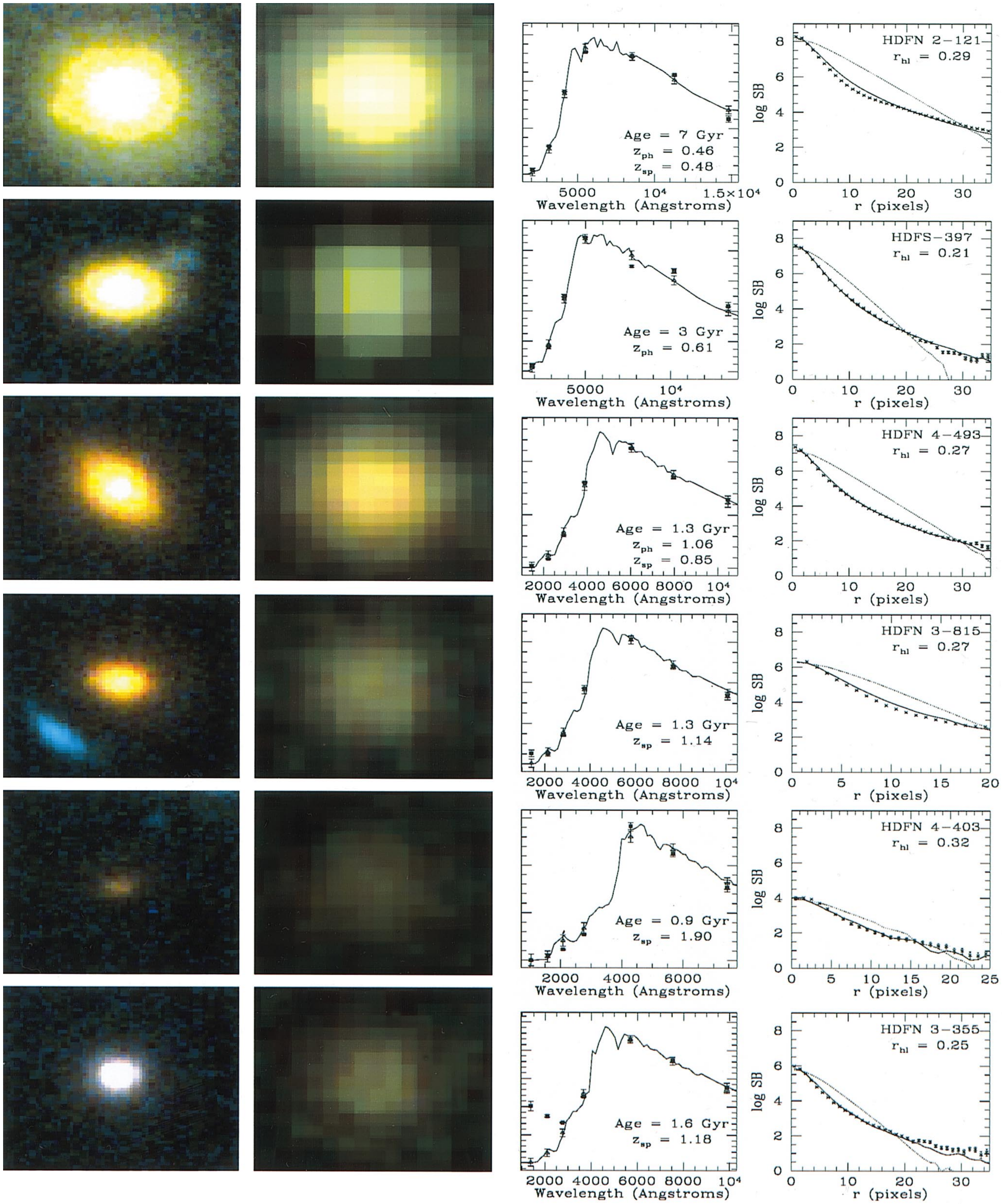

FIG. 2.—Typical spheroidal galaxies as a function of redshift. We include the optical color image, the IR (KPNO or NTT) image, the SED fits (model fluxes are given by *open triangles*) to the observations (*squares*), and the observed one-dimensional profiles (*crosses with errors*) compared to the best-fit PSF-convolved de Vaucouleurs profile (*solid line*) and exponential profiles (*dotted line*). The bottom panel shows an example of an anomalous morphologically early-type galaxy with a $U-B$ excess (see text).

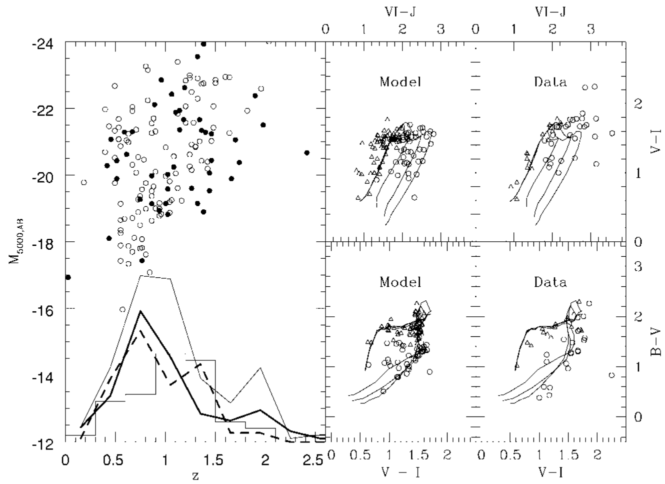

FIG. 3.—Dot plot on the left compares the redshift and absolute magnitudes (at 5000 Å) of the observations (*filled circles*) with elliptical galaxies recovered from our simulations (*open circles*; volume density here artificially increased by a factor of 2.5 to better illustrate the theoretical distribution) for our best-fit passive evolution model truncated at 2 $M_\odot$ (using the Fioc & Rocca-Volmerange 1997 spectrophotometric tables) with formation redshifts distributed between $z = 1.5$ and 2.5. The histogram shows the observed redshift distribution compared with the above best-fit model (*dashed line*) and a passive evolution model with $z_f = 3$ for two choices of geometry ($\Omega = 1$, *thick line*; $\Omega = 0.3$, *thin line*). Clearly, at most a factor of 30% decline in red galaxies is measured relative to the large volume models, but no trend to lower luminosity is found with increasing redshift. On the right, color-color diagrams are shown with evolutionary tracks indicating the sensitivity to formation redshift, z_f = 1.5, 1.75, and 2, progressing redder for later formation (*open triangles* and *open circles* denote galaxies observed at $z < 1$ and $z > 1$, respectively.)

this estimate is subject to a 50% uncertainty from the unknown volume. These conclusions are surprising given the high metal content of elliptical galaxies and implies some gas preenrichment. This requirement is more palatable in light of recent evidence of outflows in higher redshift star-forming galaxies, in particular lensed galaxies for which there is sufficient signal to detect blueshifted ISM absorption lines (Franx et al. 1997; Frye & Broadhurst 1998). Such outflows will be preferentially enriched with alpha-elements from Type II supernova (SNII) activity.

Independent of the observed outflows, Renzini (1997) has argued convincingly that SNII enrichment of the intracluster medium is indicated by the predominantly alpha-element–enriched gas. In the context of hierarchical evolution, early enriched gas will cool and fall on to the later forming, more massive halos. Locally, examples of near-solar–enriched cooling flow X-ray gas is found in groups and clusters of galaxies centered on giant elliptical galaxies of similar metallicity (Finoguenov & Ponman 1999). We suggest that cooling may be responsible for the formation of the stellar content of elliptical galaxies more generally, naturally leading to a bottom-heavy IMF consistent with our results. Inviting this simple picture is the remarkable correspondence between the most luminous X-ray cooling gas with impressively large cD galaxies (Fabian, Nulsen, & Canizares 1991). Hence it is perhaps not surprising to find that such objects contain *young* stellar populations (Mehlert et al. 1998) if this cooling gas forms visible stars. A clear test of the possible role of cooling flows in the formation of spheroidal galaxies will be provided soon by deep X-ray imaging, such as the planned *AXAF* deep field. Constraining the space density of even higher redshift red galaxies requires deeper IR imaging to explore beyond $z = 2$. The ISAAC camera on the VLT has the area and efficiency to achieve this, extending ∼2 mag fainter than the relatively low resolution ∼4 m IR imaging used here.

We thank Piero Rosati and Alvio Renzini for useful conversations. T. J. B. acknowledges NASA grant AR07522.01-96A.

REFERENCES

Barger, A. J., Cowie, L. L., Trentham, N., Fulton, E., Hu, E. M., Songalia, A., & Hall, D. 1999, AJ, 117, 102
Benítez, N., Broadhurst, T. J., Bouwens, R. J., Silk, J., & Rosati, P. 1999, ApJ, 515, L65
Bertin, E., & Arnouts, S. 1996, A&AS, 117, 393
Bouwens, R. J., Broadhurst, T. J., & Silk, J. 1998, ApJ, 506, 557
Bower, R. G., Lucey, J. R., & Ellis, R. S. 1992, MNRAS, 254, 601
da Costa, L., et al. 1999, A&A, 343, L29
Dunlop, J., Peacock, J., Spinrad, H., Dey A., Jimenez, R., Stern, D., & Windhorst, R. A. 1996, Nature, 381, 581
Faber, S., & Jackson, R. 1976, ApJ, 204, 668
Fabian, A. C., Nulsen P. E. J., & Canizares, C. R. 1991, A&A Rev., 2, 191
Fioc, M., & Rocca-Volmerange, B. 1997, A&A, 326, 950
Finoguenov, A., & Ponman, T. J. 1999, MNRAS, 305, 325
Franceschini, A., Silva, L., Fasano, G., Granato, L., Bressan, A., Arnouts, S., & Danese, L. 1998, ApJ, 506, 600
Franx, M., Illingworth, G. D., Kelson, D., Van Dokkum, P. G., Pieter G., & Tran, K. 1997, ApJ, 486, L75
Frye, B., & Broadhurst, T. 1998, ApJ, 499, L115
James, P., & Mobasher, B. 1999, preprint (astro-ph/9901401)
Kauffmann, G., & Charlot, S. 1998, MNRAS, 297, L23
Kauffmann, G., Charlot, S., & White, S. D. M. 1996, MNRAS, 283, L117
Leitherer, C., et al. 1996, PASP, 108, 996
Mehlert, D., Bender, R., Saglia, S., & Wegner, G. 1998, A&A, 332, 33
Menanteau, F., Ellis, R. S., Abraham, R. G., Barger, A. J., & Cowie, L. L. 1999, MNRAS, 309, 208
Peacock, J., Jiminez, R., Dunlop, J., Waddington, X., Spinrad, H., Stern, D., Dey, A., & Windhorst, R. 1998, MNRAS, 296, 1089
Pozzetti, L., Bruzual A., G., & Zamorani, G. 1996, MNRAS, 281, 953
Renzini, A. 1997, ApJ, 488, 35
Schweizer, F., & Seitzer, P. 1992, AJ, 104, 1039
Silva, D. R., & Bothun, G. D. 1998, AJ, 116, 85
Stanford, S. A., Eisenhardt, P. R., & Dickinson, M. 1998, ApJ, 492, 461
Stiavelli, M., et al. 1999, A&A, 343, L25
Thomas, D., Greggio, L., & Bender, R. 1999, MNRAS, 302, 537
Treu, T., et al. 1998, A&A, 340, L10
Williams, R., et al. 1996, AJ, 112, 1335
Worthey, G. 1994, ApJS, 95, 107
Zepf, S. 1997, Nature, 390, 377